Supplemental Experimental Procedures

Cloning

The retroviral SIN-TRE-GFP-miR30-PGK-Puro (TGMP) vector was generated from the SIN-TRE-PIG vector (Dickins et al., 2005). PCR-generated GFP and miR30 fragments were digested them with SalI or AgeI/BamHI respectively, and cloned into SIN-TRE-PIG digested with XhoI/EcoRV, yielding SIN-TRE-GFP-miR30 (TGM). Next, the TGM vector was digested with *Bgl* II/ *BamHI* restriction enzymes and ligated into MSCV-PGKpuro-SIN. Knockdown efficiency was assessed following retroviral transduction into primary mouse embryonic fibroblasts (MEFs) expressing tTA. To generate the pColTGM flp-in vector, a GFP-miR30 PCR fragment from TGMP was ligated into pBS31 with a destroyed XhoI site (Beard et al, 2006) and 116-bp XhoI-EcoRI DNA fragments encoding shRNAs targeting p53, INK4a/ARF, ARF, APC and luciferase (listed in Table S2) were subcloned into pCol-TGM.

Small RNA isolation, cloning and bioinformatic analysis

RNA was extracted, purified, cloned and analyzed as previously described (Malone et al., 2009), using TRIZOL® reagent (Invitrogen™), followed by phenol/choloroform/isoamyl alcohol and chloroform purifications. After 5' and 3' adapter ligations and PCR, 18-29nt small RNA libraries were sequenced on the Illumina®/Solexa™ platform. Sequence reads were clipped and redundant sequences collapsed; any sequencing artifacts (unclipped or low-complexity sequences) were removed from further analysis, along with structural RNA degradation products from tRNAs, rRNAs, snoRNAs, snRNAs and smRNAs. The number of remaining sequences was scaled to determine normalization factors for cross-comparison of all libraries. Remaining sequences were then mapped against the latest *Mus musculus* miRBase catalog (http://www.mirbase.org/), and the full-length luciferase shRNA vector sequence to determine miRNA abundances in all sequenced

libraries. Annotated sequencing reads were then scaled for subsequent analysis, using the determined normalization factors.

Image acquisition and manipulation

Brightfield images of cells were captured on a Nikon TE2000-S inverted microscope (Nikon, Tokyo, Japan) using a 10X objective (Nikon, NA 0.3) and a Spot Insight QE CCD camera (Diagnostic Instruments, Sterling Heights, MI). Fluorescence and H&E stained sections were imaged on a Zeiss Axioscope Imager Z.1 using a 10x (Zeiss NA 0.3) or 2.5x (Zeiss NA 0.06) objective and an ORCA/ER CCD camera (Hamamatsu Photonics, Hamamatsu, Japan). H&E photographs for the lymphoma experiments were taken on a Nikon Eclipse 80i microscope with a Nikon Digital Sight camera using NIS-Elements F2.30 software at a resolution of 2560×1920. Whole embryo brightfield and GFP fluorescence images were acquired on a Nikon SMZ1500 dissecting scope equipped with a DXM1200F CCD camera (Nikon). For bioluminescence imaging, mice were anesthetized with isoflurane, and ventral hair removed using Nair. Topical application to the ventral area was performed using felt applicators soaked in a luciferin-DMSO solution (5.6mg/ml in 40% DMSO-PBS). Bioluminescent imaging was performed 10 min following luciferin-DMSO treatment using an IVIS100 imaging system (Caliper LifeSciences). Tissues and embryos were submerged in luciferin-DMSO prior to imaging. *Image manipulation:* Raw .tif files were processed using Image J freeware (rsb.info.nih.gov/ij) and Photoshop CS2 software (Adobe Systems Inc., San Jose, CA) to measure greyscale levels and apply false coloring.

Supplemental Figure Legends

Figure S1. Flp/FRT Recombinase mediated cassette exchange at the *ColA1* locus in KH2 mES cells and testing functional gene knockdown ES cells. Relates to Figure 1.

(A) Schematic representation of the downstream region of the *ColA1* locus after placement of an frt-hygro-pA "homing" cassette by homologous recombination. The "FRT homing cassette" consists of PGK-Neo^R and a hygromycin resistance cassette with no ATG start codon or promoter. Coelectroporation of the pColTGM and pCAGs-Flpe recombinase vectors promotes inter- and intrachromosomal recombination at the *ColA1* locus downstream of the Type I Collagen gene, resulting in excision of PGK-Neo^R and integration of the pColTGM. Correct integration confers hygromycin resistance.

(B) Representative Southern blot analysis of hygromycin resistant-GFP positive (DOX treated) clones using a ColA1 probe (Beard et al., 2006). DNA was digested with SpeI.

(C) Southern blot analysis of transgenic animals generated by pronuclear injection (left 4 lanes) and Flp/FRT RMCE (right 4 lanes) using a GFP probe to identify all integrations. DNA was digested with EcoRI.

(D) Histograms indicating the presence of GFP negative cells in untargeted KH2 (left) and TG-p53.1224 ES cells off DOX (right) and GFP positive TG-p53.1224 ES cells on DOX.

(E) DOX-treated p53.1224/R26-rtTA ES cells exhibit impaired DNA damage response. R26-rtTA ES cells with either p53.1224 or luc.1309 were pre-treated with or without DOX for 4 days, then subjected to increasing concentrations of Adriamycin (0.4-256 ng/ml). Cell viability was assessed 18hr post Adriamycin treatment by propridium iodide staining and FACs analysis.

(F) DOX-induced repression of *Pou5f1* in Oct.468/Rosa-rtTA ES cells promotes differentiation toward the trophoectoderm lineage. Quantitative PCR analysis of markers of trophoectoderm (cdx2, Hand1, dlx3 KDR) and embryonic stem cells (Errb and Nanog).

Table S1. Schematic overview of transgenic ES cell production. Relates to Figure 1.

Details of the high throughput workflow to generate targeted ES cell clones. One confluent 6cm plate of KH2 ES cells can be used for 4 separate electroporations to generate unique ES cell lines. Immediately following electroporation, a small fraction of ES cells were plated in normal or DOX-containing media for GFP expression by FACs analysis 48 hours later to assess electroporation efficiency. If FACs revealed greater than 10% GFP positive cells, the cells were plated in hygromycin-containing media (140μg/ml) for 10-14 days until colonies were visible. For each independent electroporation, 4-6 clones were picked and expanded for functional knockdown analyses and mice production.

Figure S2. Reversible knockdown of gene targets in primary mouse embryonic fibroblasts derived from *ColA1*-TGM ES-cell derived mice. Relates to Figure 2.

(A,B) Western blot analysis of MEFs harvested from a cross between C57BL/6 WT mice and TG-p16/p19.478/R26-rtTA (A) or TG-APC.9363/R26-rtTA (B) founder mice, DOX-treated as indicated.

(C) DOX-induced repression of *APC* in TG-APC.9363/R26-rtTA MEFS induces Axin2 expression. Quantitative PCR analysis of Axin2 following DOX treatment and withdrawal.

Figure S3. Endogenous miRNA levels are unaffected by exogenous shRNA induction. Relates to Figure 3.

Scatter plot representing the normalized expression of the 319 most abundant miRNAs from DOX-treated and untreated TG-luc.1309 MEFs.

Figure S4. DOX-dependent knockdown in GFP-marked organs of Rosa-rtTA and CAGs-rtTA3 mice. Relates to Figure 4.

(A) Representative GFP and bioluminescent images of organs harvested from untreated and DOX-treated shluc/R/RL mice.

(B, C) GFP intensity and bioluminescence quanitfication of organs harvested from untreated and DOX-treated mice. Error bars represent SEM, n=3.

(D) Representative GFP and bioluminescent images of organs harvested from untreated and DOX-treated shluc/CAGs-rtTA3/RL mice.

(E, F) Relative GFP intensity and bioluminescence of organs harvested from untreated and DOX-treated mice. Error bars represent SEM, n=3.

Figure S5. APC depletion causes multiple defects during embryonic and juvenile development. Relates to Figure 5.

(A) GFP fluorescent images of E14.5 embryos treated with DOX from E8.5.

(B) Brightfield images of Alcian blue / Alizarin red stained E14.5 skeletons from TG-luc.1309/R26-rtTA and TG-APC.9365/R26-rtTA double transgenic embryos. TG-APC.9365 mice show a severe block in development of multiple skeletal tissues.

(C) Alcian blue and Alizarin red stained images are from TG TG-luc.1309/R26-rtTA$^{T/T}$ and TG-APC.9365/R26-rtTA$^{T/T}$ E18.5 embryos.

(D) Brightfield images of embryos and Alcian/Alizarin stained skeletons showing duplication of the digits in the forelimbs of TG-APC-3374 mice pulsed with DOX from E8.5-E12.5.

(E) Representative photographs of TG-luc.1309/R26-rtTA and TG-APC.9365/R26-rtTA at P18, on DOX 1 day before birth.

(F) Western blot of whole cell lysates taken from purified intestinal villi treated with or without DOX for different times as indicated.

Figure S6. APC depleted T lymphoblastic leukemia/lymphoma causes malignant disease in transplanted recipient mice. Relates to Figure 6.

(A) Representative flow cytometry plots from peripheral blood of TG-APC.3374 lymphoma transplanted SCID mouse. All GFP positive (lymphoma) / CD45 positive cells express both CD4 and CD8

(B) GFP fluorescent photograph of TG-APC.3374 lymphoma transplanted SCID mice maintained on DOX or removed from DOX treatment for 2 weeks. GFP marks the presence of leukemia/lymphoma.

(C) Western blot of whole cell lysates from TG-APC.9365 and TG-APC.3374 primary lymphomas (left), tumors from transplanted animals on DOX (middle) and relapse tumors from transplanted animals removed from DOX for 4 weeks (right).

Figure S7. Reversible suppression of ARF in a multi-allele disease model documents a contribution to tumor maintenance. Relates to Figure 7.

(A) Serial bioluminescence images of *shARF/Kras* mice treated with adeno-CRE and DOX at 4-6 weeks of age. At 8 w.p.i., cohorts were randomized and followed with or without DOX treatment for 2 weeks.

(B) Quantification of lesions present in the lungs *shARF/Kras* mice at 8 and 10 w.p.i. either on or off DOX. For each animal, area and multiplicity represent the mean scored across 10 H&E stained sections taken at 100 microns apart. Error bars represent SEM (left) and mean (right)

(C) Macroscopic brightfield and GFP images of whole lungs isolated from *Kras* and *shARF/KRas* mice 12 w.p.i. Arrows indicate surface tumor nodules.

(D) H&E stained sections of the lungs from *shARF/KRas* mice 12 w.p.i. demonstrating Grade I (well-differentiated), II (moderately-differentiated) and III (poorly differentiated) adenocarcinomas present. Arrow (right) marks multinucleated cell characteristic in grade III adenocarcinomas. Scale bar = 200μm (left), 100μm (middle, right).

(E) Representative H&E stained sections of the lungs from *Kras* and *shKRas* mice. Scale bar = 5mm.

(F) Confocal immunofluorescence microscopy images of 150 micron sections from lungs of *shRen/Kras* and *shARF/Kras* animals on DOX at 8 w.p.i. or off DOX for 2 weeks at 10 w.p.i. Sections were stained with an antibody to detect Cleaved caspase 3 and DAPI.

Supplemental Figure

Figure S1

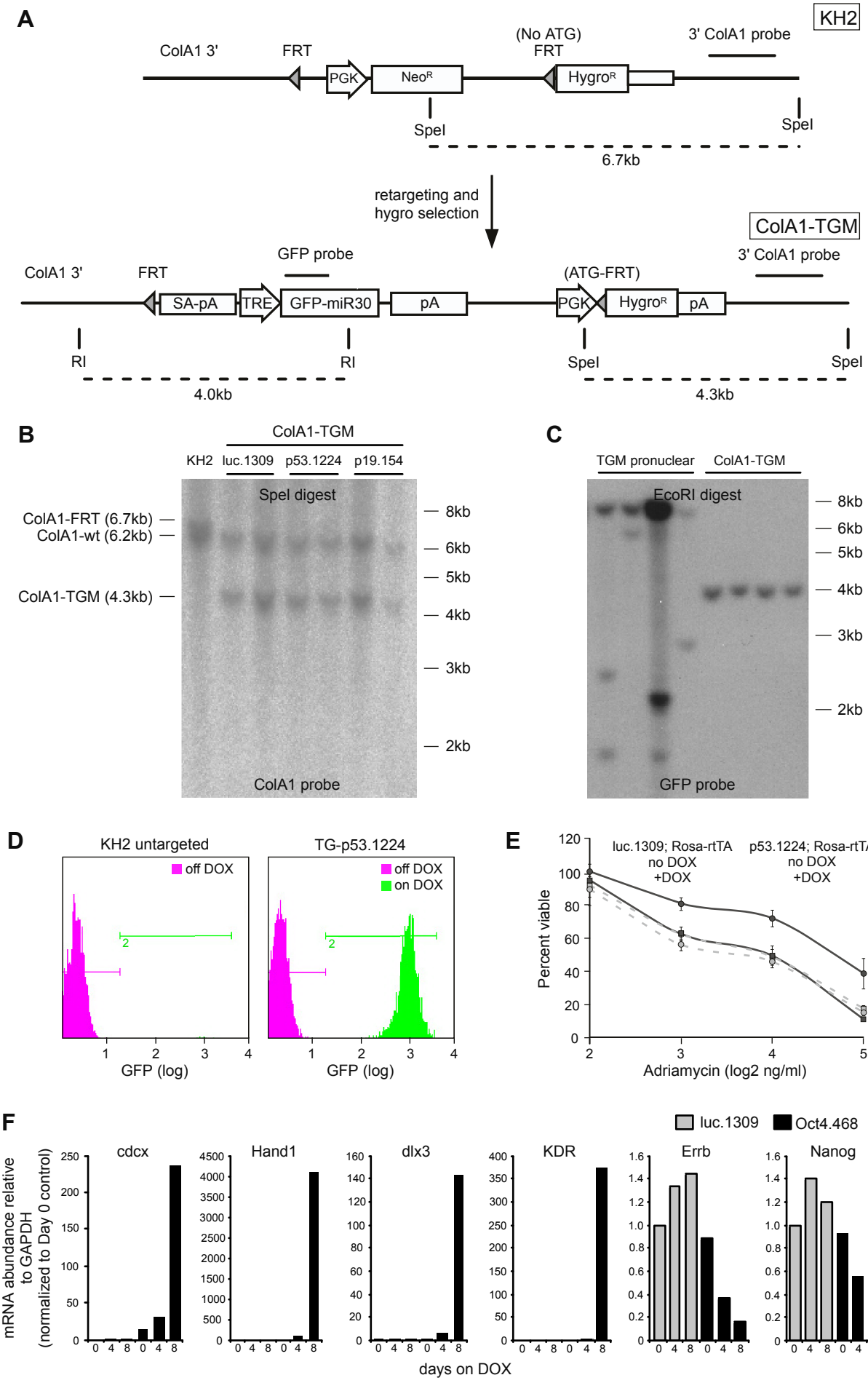

Supplemental Figure

Figure S2

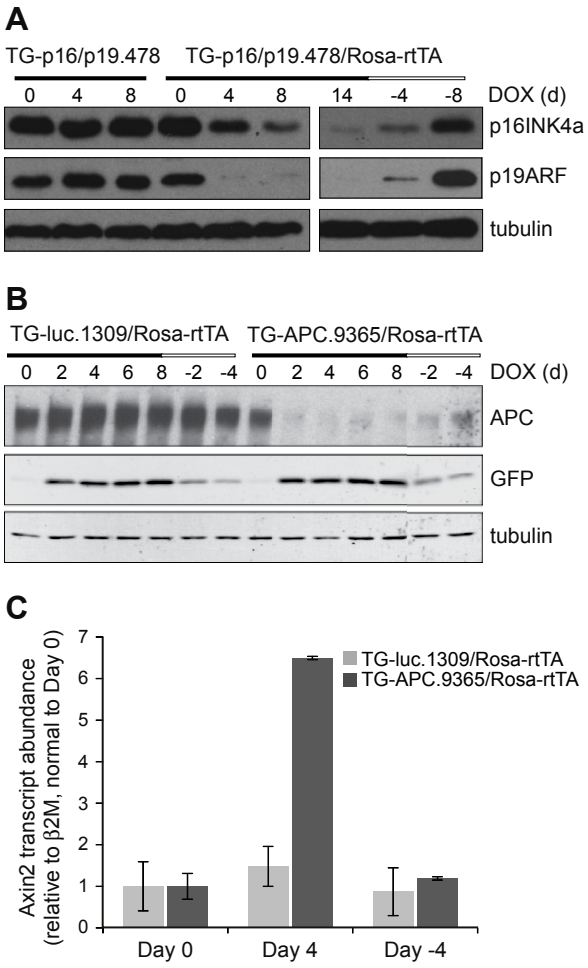

Supplemental Figure

Figure S3

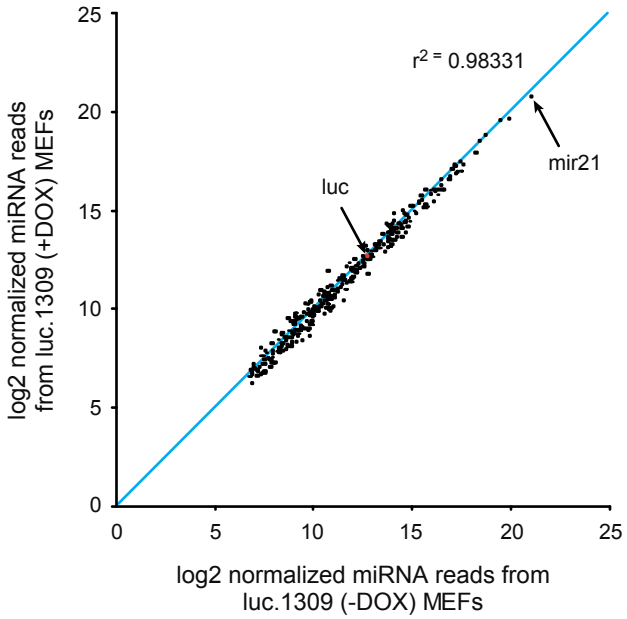

Supplemental Figure

Figure S4

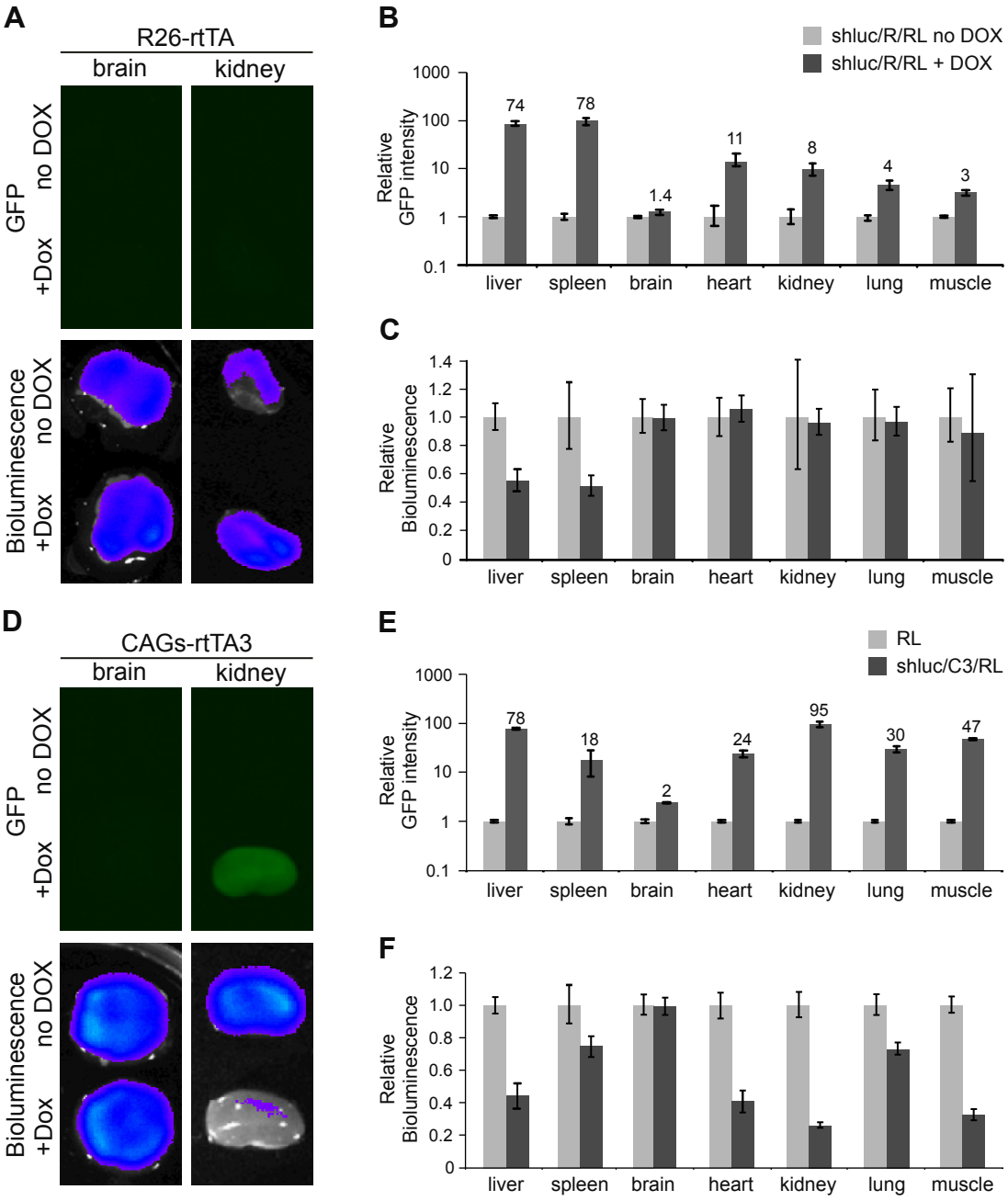

Supplemental Figure

Figure S5

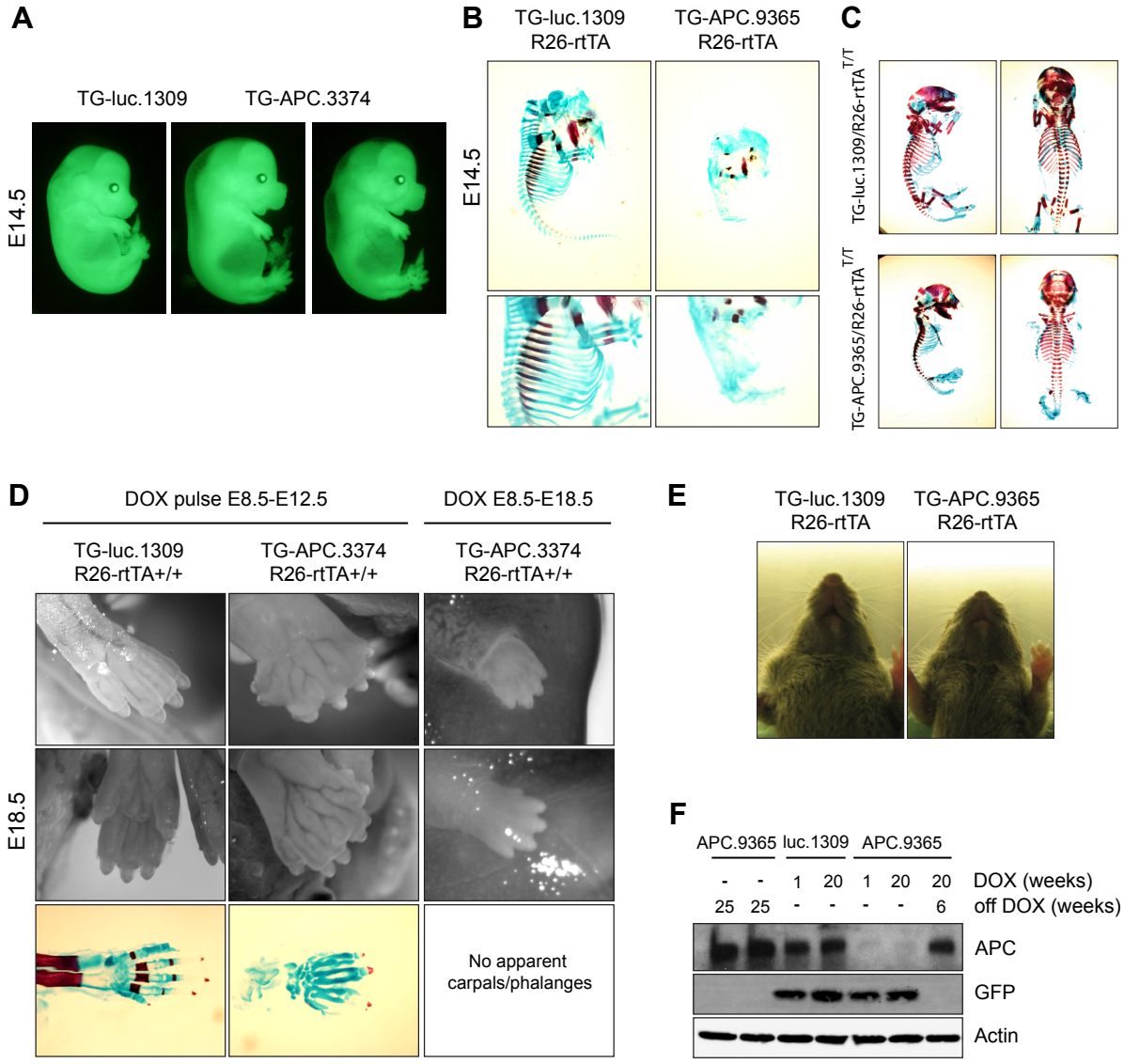

Supplemental Figure

Figure S6

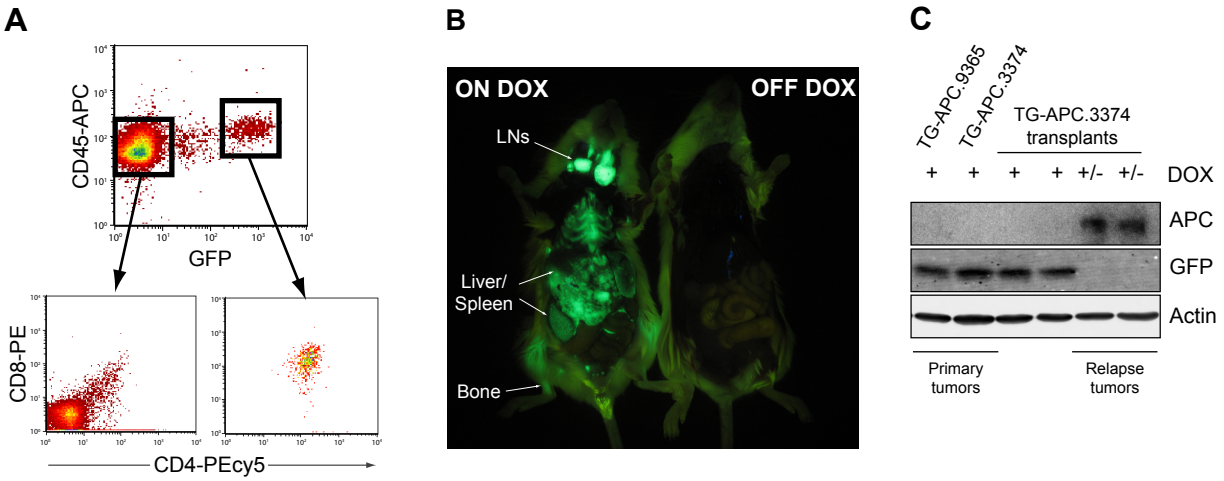

Figure S7

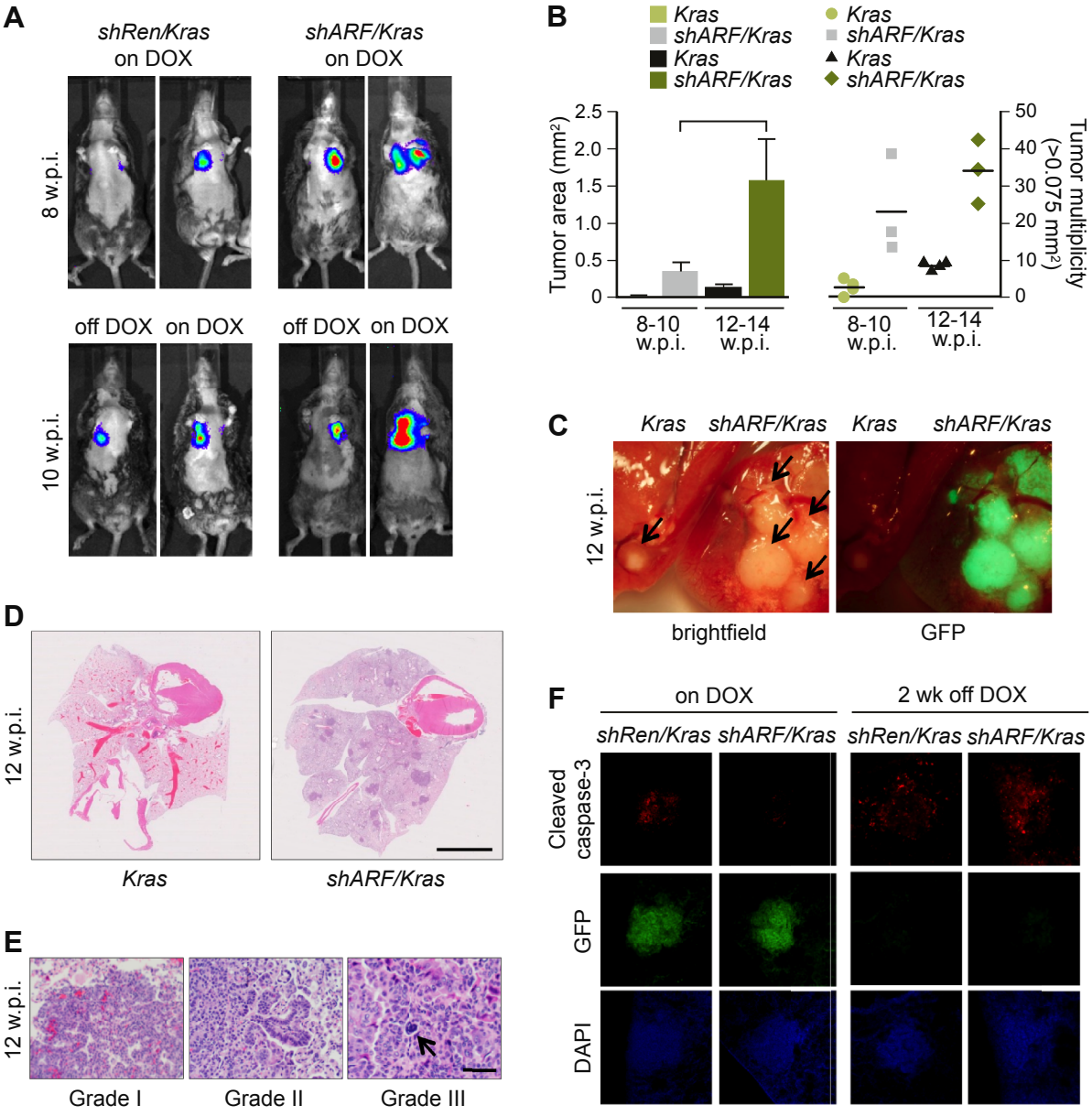
A
shRen/Kras on DOX
shARF/Kras on DOX
8 w.p.i.
off DOX on DOX
off DOX on DOX
10 w.p.i.
B
Kras
shARF/Kras
Kras
shARF/Kras
Kras
shARF/Kras
Kras
shARF/Kras
Tumor area (mm²)
2.5
2.0
1.5
1.0
0.5
0
8-10 w.p.i.
12-14 w.p.i.
50
40
30
20
10
0
Tumor multiplicity (>0.075 mm²)
8-10 w.p.i.
12-14 w.p.i.
C
Kras
shARF/Kras
Kras
shARF/Kras
12 w.p.i.
brightfield
GFP
D
12 w.p.i.
Kras
shARF/Kras
E
12 w.p.i.
Grade I
Grade II
Grade III
F
on DOX
2 wk off DOX
shRen/Kras
shARF/Kras
shRen/Kras
shARF/Kras
Cleaved caspase-3
GFP
DAPI